

The case $l=0$ is, written out explicitly,

$$v_0(k,\lambda) = -\frac{e^{-ka}}{2\pi^2 k\lambda} \frac{(\lambda \cos\lambda a + k \sin\lambda a)}{(k^2 + \lambda^2)}.$$

ACKNOWLEDGMENTS

I would like to thank Professor H. Feshbach and Professor F. Villars for listening patiently and offering suggestions at various stages in the development of this paper, and to Dr. S. C. Wang for his help in solving the integral equations described herein.

PHYSICAL REVIEW

VOLUME 115, NUMBER 6

SEPTEMBER 15, 1959

Elastic Scattering of Protons by Nitrogen

A. J. FERGUSON, R. L. CLARKE, AND H. E. GOVE
Atomic Energy of Canada Limited, Chalk River, Ontario, Canada
 (Received October 7, 1958)

The cross sections for the elastic scattering of protons by nitrogen have been measured in 105 angular distributions ranging in angle from 53° to 155° and in energy from 1.05 Mev to 2.93 Mev. Resonances have been observed at 1065±5 kev, 1557±6 kev, 1743±7 kev, 1803±7 kev, 2344±10 kev, and 2468±10 kev.

INTRODUCTION

THE elastic scattering of protons by nitrogen in the energy range covered by electrostatic accelerators shows, in addition to a number of well-established resonances, a large background of potential scattering. It has been reported from 0.6 Mev to 4.1 Mev in several recent papers.¹⁻⁴ Spin and parity assignments have been found for the resonances at 1.065 Mev and 1.557 Mev. The lack of knowledge of the background scattering, on which the emphasis of the present work rests, has been the principal obstacle to establishing the assignments for the others. An early report⁵ that the *P*-wave potential phase shifts were small below 2.0 Mev has been found incorrect. This conclusion arose from an incorrect normalization for the cross sections, which were about 10% too low. The cross sections of Tautfest and Rubin⁶ are approximately the same as those of reference 5. Hagedorn *et al.*² have compared these results with the more recent data and show that they are consistently low. The results of the present work are available in tabular form in an unpublished report.⁷ The present data, which are in agreement with the

recent data^{1,2} cannot be satisfactorily analyzed with *S*-waves only and thus imply the presence of *P*-waves and possibly higher ones. A phase shift analysis of these results which includes *P*-waves is described in the following paper.⁸

APPARATUS

The proton beam for the work was supplied by the Chalk River electrostatic accelerator. The upper limit to the proton energy available was 3 Mev. The lower limit was about 1 Mev, which was the minimum energy where a resolved peak in the spectrum from the scintillation proton counter could be obtained. The energy of the proton beam was measured by deflecting it through 90° in a uniform magnetic field which, in turn, was measured and controlled by a proton gyromagnetic resonance detector.

The scattering chamber is shown in Figs. 1 and 2.

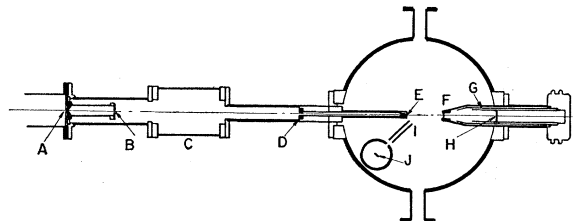


FIG. 1. Gas scattering chamber. *A*, *B*, and *D* are collimating apertures. *E* and *F* are thin nickel windows for beam entry and exit. *F*, *G*, and *H* are the beam catcher assembly. *I* is the counter collimator and *J* a small scintillator for particle counting mounted on the rotating cover.

¹ Bolmgren, Freier, Likely, and Famularo, *Phys. Rev.* **105**, 210 (1957).

² Hagedorn, Mozer, Webb, Fowler, and Lauritsen, *Phys. Rev.* **105**, 219 (1957).

³ Bashkin, Carlson, and Jacobs, *Bull. Am. Phys. Soc. Ser. II*, **1**, 212 (1956).

⁴ Olness, Vorona, and Lewis, *Bull. Am. Phys. Soc. Ser. II*, **2**, 53 (1957).

⁵ Gove, Ferguson, and Sample, *Phys. Rev.* **93**, 928(A) (1954).

⁶ G. W. Tautfest and S. Rubin, *Phys. Rev.* **103**, 196 (1956).

⁷ Ferguson, Clarke, Gove, and Sample, Atomic Energy of Canada Report PD-261, 1956 (unpublished).

⁸ A. J. Ferguson, following paper [*Phys. Rev.* **115**, 1660 (1959)].

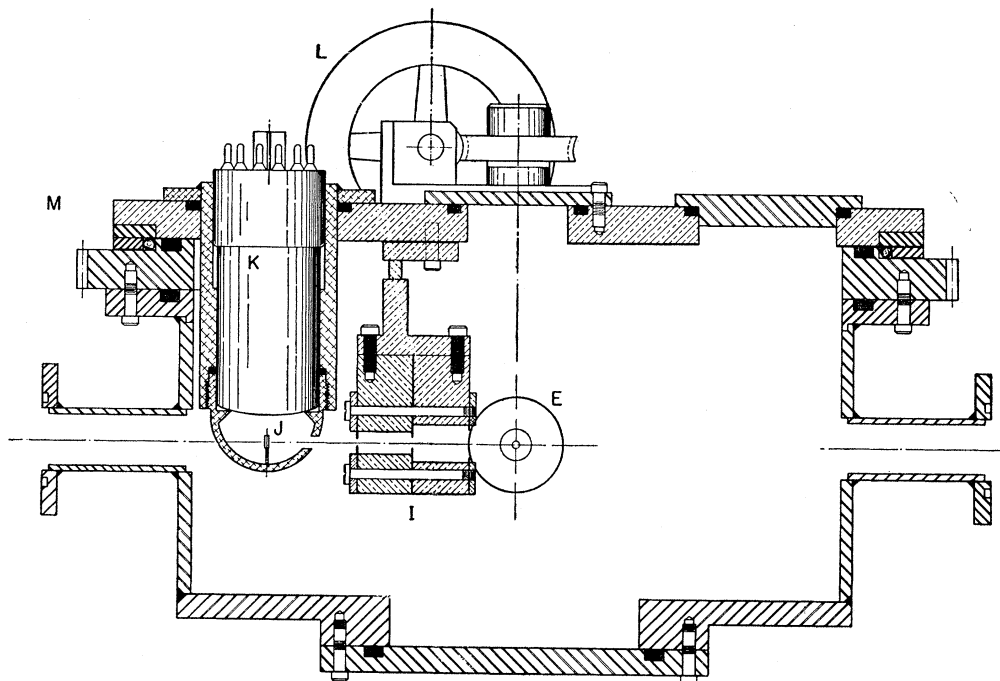


FIG. 2. Vertical section of the gas scattering chamber perpendicular to the beam axis showing the photomultiplier, *K*, and counter collimator mounting.

It is essentially a large scattering chamber similar to those described by Blair *et al.*⁹ and Herb *et al.*¹⁰ Its main feature is the use of a large rotating lid which allows electrical connection to be made directly to the photomultiplier. This avoids the difficulty of electrical discharges from the high voltage lead to the counter occurring in the low pressure target gas.

Figure 1 shows a horizontal section of the chamber at the beam axis. Apertures *A* and *D* collimate the incident proton beam. These are circular holes of diameter 0.089 in. in 0.04 in. thick tantalum sheet and are separated by 20 in. Aperture *B* is a "scraper" to suppress particles scattered by the edges of the first one. A gas tight metal foil is located at *E* about one in. from the center of the chamber. This foil separates the target gas from the vacuum of the accelerator. The foils used

were of nickel, 40 $\mu\text{g}/\text{cm}^2$ or 80 $\mu\text{g}/\text{cm}^2$ in thickness. Earlier work with 250 $\mu\text{g}/\text{cm}^2$ mica foils indicated that these introduced a straggling of the beam of about 15 keV, which is intolerable for the present work. Even the thin nickel is believed to cause 1 or 2 keV of straggling. *C* is a flap valve which permitted the chamber to remain under vacuum when disconnected from the beam tube of the accelerator.

The counter assembly is mounted on the rotating lid. It consists of a small potassium iodide scintillator *J* about $\frac{1}{16}$ in. thick by $\frac{1}{4}$ in. square mounted on a Lucite post. The light pulses from this are picked up by a 5819 photomultiplier, *K*, shown in Fig. 2. Below the scintillator is a polished aluminum hemispherical reflector to improve the light collection. *I* is the counter collimator which defines the target region by the intersection of its acceptance angle with the beam. The two extreme rays defined by the collimator in the plane of scattering have an angular separation of 6.4° . The mean spread in scattering angle will be somewhat less than this. An O-ring vacuum seal between the glass envelope of the photomultiplier and the housing for it permits the photosensitive cathode to be near the scintillator. The counter collimator was aligned optically. For this, the counter and beam catcher were removed and the lid was rotated to the zero angle. The alignment of the collimator could be checked and adjusted by sighting through it into the beam collimator. The zero setting was found to be reproducible to within $\pm 0.1^\circ$ by this procedure. The angular distribution of a pure Ruther-

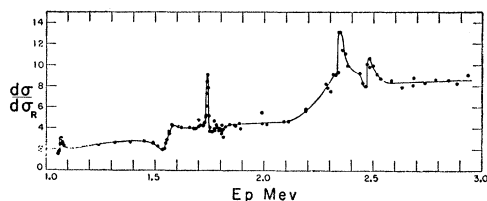


FIG. 3. Yield curve at the maximum angle of scattering. The yield is normalized to that from a pure Rutherford scatterer. E_p is the energy of the incident protons in the laboratory system.

⁹ Blair, Freier, Lampi, Sleator, and Williams, Phys. Rev. **74**, 553 (1948).

¹⁰ Herb, Kerst, Parkinson, and Plain, Phys. Rev. **55**, 998 (1939).

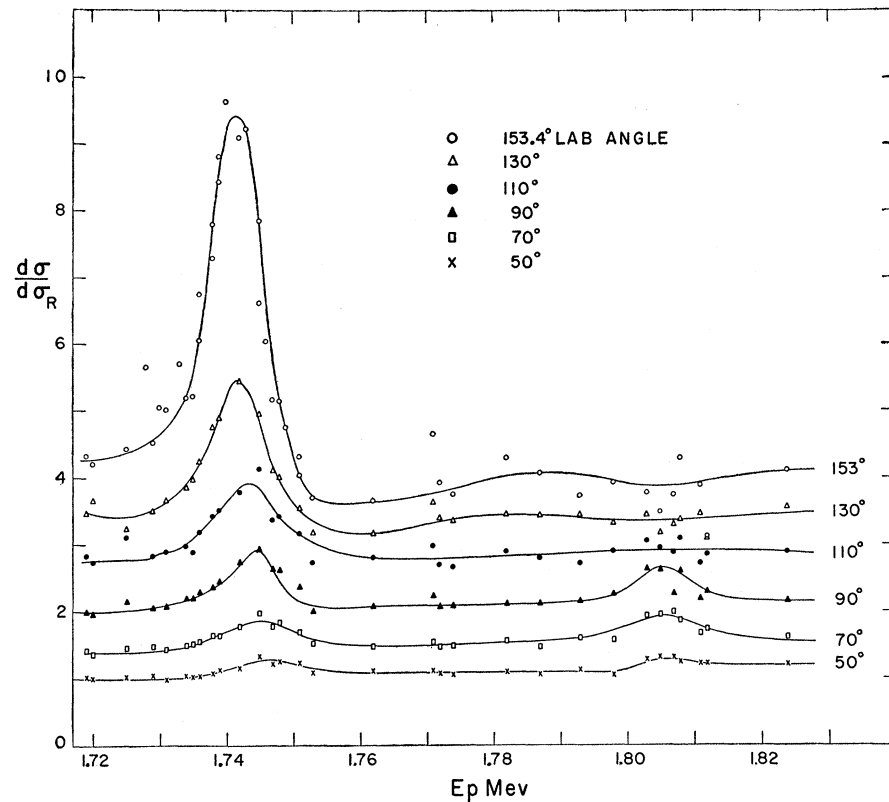


FIG. 4. Yield curves at six angles near the 1.743-Mev and the 1.803-Mev resonances.

ford scatterer provided another check of the accuracy of the angle measurements. The lid is supported at M on a complete ring of ball bearings. Just within this is the O-ring seal to maintain the internal vacuum. Two hand wheels, L , turn the rotating lid through worms and sprockets that engage a gear cut around the top flange of the chamber.

After traversing the target region, the proton beam enters the beam catcher through another nickel window F , of thickness $200 \mu\text{g}/\text{cm}^2$, situated 2 in. from the center of the chamber. The catcher has two electrodes in it. The inner, H , is a Faraday cup to collect the beam, the end of which is a quartz disk lightly aluminized on one side. This made the proton beam visible through the Lucite end plate of the catcher and was helpful in getting it lined up along the axis of the collimator. The outer, G , is an electrode biased to -300 v to suppress the escape of electrons from the cup and the collection of electrons from the gas and window. The entire catcher assembly was evacuated by a small fractionating oil diffusion pump. A current to the negative electrode was observed which was normally about 5% of the current to the collector cup. Since ion currents in the electron trap can affect the measurement of the beam current, a test was made for this source of error. A comparison was made between the counts of scattered particles at a fixed angle and energy and for a specific accumulated proton current

first when the beam catcher was evacuated by the diffusion pump and second with it at forevacuum pressure. The difference between the counts was negligible, indicating that the contribution from ion currents was not significant.

Calibration of the energy scale was done by placing a thick LiF target in the center of the chamber and evacuating all gas but retaining the entry foil at E . Then from the observed threshold of the $\text{Li}^7(p,n)\text{Be}^7$ reaction, the energy scale provided by the beam analyzing magnet was calibrated, using 1.882 Mev for this threshold.¹¹ A correction was made for energy loss in the gas between the window and the target region. The energy of the 1.743-Mev resonance was fixed in this scale and it was then used as a secondary standard in other runs. The accuracy of the energy is about 0.3%. The stability of the beam for the duration of an angular distribution measurement was $\pm 2 \text{ kev}$.

The pressure of the gas in the chamber was measured on a manometer containing butyl phthalate vacuum oil. Pressures ranged from 20 cm of oil used in a few early measurements down to 4 cm and 2 cm in the later work. The error of reading the manometer was deemed to be 0.1 mm of oil, which constitutes generally the largest source of error in the work. Typical values for the errors arising from various sources of uncertainty are: counting statistics 2%, pressure measurement 3%,

¹¹ Herb, Snowdon, and Sala, Phys. Rev. **75**, 246 (1949).

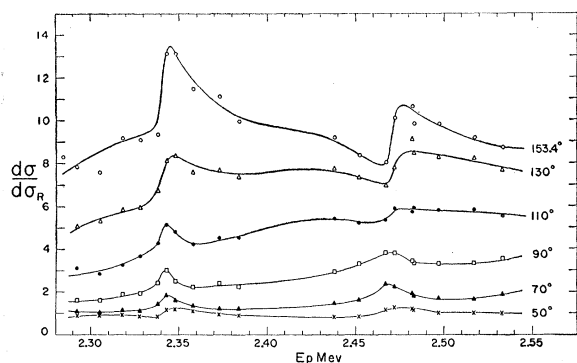


FIG. 5. Yield curves at six angles near the 2.344-Mev and 2.468-Mev resonances.

argon calibrations 3%, beam measurement 2%, gas impurities $\frac{1}{2}$ %, and the angle measurement $\frac{1}{2}$ %. The tabulation of reference 7 gives the estimated error of each point.

EXPERIMENTAL RESULTS

The bulk of the experimental data consists of 105 angular distribution measurements taken for incident proton energies ranging from 1.05 Mev to 2.94 Mev. There are, in addition, a number of yield curves taken

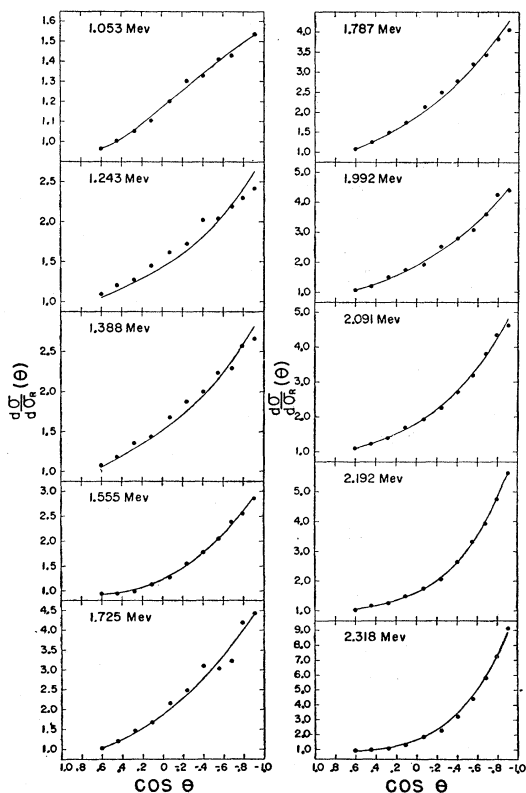


FIG. 6. Typical angular distributions between 1.05 Mev and 2.32 Mev. The solid line is the theoretical curve from the phase shift analysis of reference 7.

at the maximum available scattering angle of 155.2° (center-of-mass system). All of the cross sections have been normalized to the Rutherford differential cross section as described below. The accuracy of the results is generally about 5%. A yield curve at the largest angle is shown in Fig. 3. Open circles denote the data taken from yield curves, and crosses those taken from angular distributions. The energy of the incident protons, E_p , is always given for the laboratory system. In Figs. 4 and 5 are plotted data for the region near 1.79 Mev and 2.4 Mev as a set of yield curves for the center of mass angles 53.1° , 73.9° , 94.1° , 113.9° , 133.1° , and 155.2° . These show the constant angle contours for the resonances 1.743 Mev, 1.803 Mev, 2.344 Mev, and 2.468 Mev. Figures 6 and 7 show some typical angular distributions. The solid lines are theoretical curves based on the phase shift analysis of the following paper.

The angular range covered was from 53.1° to 155.2° (c.m.) in approximately 10° steps for most of the runs, although a few runs extend in angle down to 27.8° . In measuring a distribution, the procedure was to start

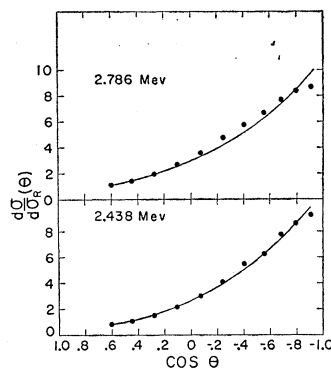


FIG. 7. Typical angular distributions between 2.4 Mev and 2.93 Mev. The solid line is the theoretical curve from the phase shift analysis of reference (7).

at the maximum angle and to proceed to the minimum taking every second angular position and then to return to the maximum filling in the omitted steps and finally repeating the measurement at the maximum. This procedure was designed to reveal systematic changes that occurred in the course of a distribution, and a number of runs have been rejected from inconsistencies revealed in this way.

The yield of scattered particles in the laboratory system may be written

$$Y = \frac{Fn\ell A}{G} \frac{d\sigma_R}{d\Omega},$$

where F is the incident flux in particles per second, n the number of scattering centers per cm^3 , ℓ the target thickness in cm, $A = d\sigma/d\sigma_R$, the ratio of the actual differential cross section to the Rutherford cross section, G is the ratio between the yield in the center-of-mass system and the laboratory system,¹² and $d\sigma_R/d\Omega$ is the Rutherford scattering cross section.

¹² J. P. Marion and A. S. Ginzburg, Atomic Energy Commission Report NP-6241 (unpublished).

We write $t=w/\sin\varphi$, where φ is the scattering angle in the laboratory system and w the width of the beam accepted by the detector. We have also

$$\frac{d\sigma_R}{d\Omega} = \left(\frac{Ze^2}{2Mv^2} \right)^2 \csc^4(\vartheta/2),$$

where Z is the charge number of the target element, M the reduced mass of the system, v the velocity of the incident particle relative to the target and ϑ the scattering angle in the center-of-mass system. It is evident that the quantity $(Y/A)E^2 \sin\varphi \sin^4(\vartheta/2)$ is independent of angle and the energy, E . By substituting in the scattering chamber a gas known to obey the Rutherford law, this constant, and consequently A , can be evaluated. If the quantity $YE^2G \sin\varphi \sin^4(\vartheta/2)$ is independent of E and ϑ , then this is virtually conclusive evidence that pure Rutherford scattering is obtained, i.e., that $A=1$, since the departures that can occur vary irregularly with energy and angle. Argon has been found satisfactory at energies below 1.9 Mev. We have observed a cluster of narrow resonances at 1.9 Mev and a broad one at 2.5 Mev, making these regions unacceptable for calibration purposes. Figure 8 shows a typical angular distribution for argon at 1.573 Mev in which the angular dependence has been corrected as in the foregoing.

The resonances observed in this work have energies: (1065 ± 5) kev, (1557 ± 6) kev, (1743 ± 7) kev, (1803 ± 7) kev, (2344 ± 10) kev, and (2468 ± 10) kev. These agree well on the whole with the recent work.^{1,2}

There is some disagreement with Hagedorn *et al.*² regarding the width of the 1.55-Mev resonance. On the

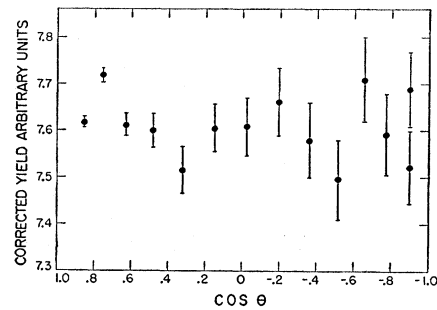


Fig. 8. Angular distribution for argon gas at 1.573 Mev. Each point has been corrected by the appropriate angle dependent factor required in normalizing to the yield of a Rutherford scatterer. The errors shown are those due to counting statistics.

basis of fits at 154° , 125° , and 90° these workers give 34 ± 4 kev for this width. Gove, Ferguson, and Sample⁵ reported 53 kev based on a fit at 155° only. Both of these have ignored the variation of the nonresonant scattering. Some attempts have been made to fit the 155° cross section data assuming that the S -wave potential scattering is given by the average course of the $\delta^{3/2+}$ phase shift curve derived in the following paper.⁶ These have not been satisfactory for either 34 kev or 53 kev for the width, but they suggest that the first figure is too low.

ACKNOWLEDGMENTS

Dr. J. T. Sample assisted us in making many of the measurements. We are indebted to the Minnesota group for supplying us with a table of their cross sections. Much credit is due to the operating staff of the accelerator for their efficient handling of the machine.